2014 IEEE International Conference on Robotics & Automation (ICRA)
Hong Kong Convention and Exhibition Center
May 31 - June 7, 2014. Hong Kong, China

Stability and control of a quadrocopter despite the complete loss of one, two, or three propellers

Mark W. Mueller and Raffaello D'Andrea

***Abstract*— This paper presents periodic solutions for a quadrocopter maintaining a height around a position in space despite having lost a single, two opposing, or three propellers. In each case the control strategy consists of the quadrocopter spinning about a primary axis, fixed with respect to the vehicle, and tilting this axis for translational control. A linear, time-invariant description of deviations from the attitude equilibrium is derived, allowing for a convenient cascaded control design. The results for the cases of losing one and two propellers are validated in experiment, while the case of losing three propellers is validated in a nonlinear simulation. These results have application in multicopter fault-tolerant control design, and also point to possible design directions for novel flying vehicles.**

I. Introduction

Multicopters have found broad use as research platforms, used e.g. for vision based pose estimation with quadrocopters [1] and hexacopters [2], and also as platforms allowing for new capabilities. For example, the use of both quadrocopters and hexacopters for whale monitoring is investigated in [3], and hexacopters are used in [4] for weed research; a team of quadrocopters is used to carry a slung load in [5] and an octocopter is used to calibrate radio telescope antennae in [6].

Amongst others, a motivation for using a multicopter with six or more propellers, instead of a four propeller quadrocopter, is that the vehicle is able to maintain normal flight if one of the propellers fails (see e.g. [7] for a hexacopter design and [8] for an octocopter rotor failure strategy). A survey on research on fault detection and diagnosis and fault-tolerant control strategies for unmanned rotary wing vehicles is given in [9], and an example of currently available commercial solutions are the emergency parachutes of [10].

Partial failure of a quadrocopter actuator is investigated for example in [11], [12] and [13]. A complete propeller failure for a quadrocopter is investigated in [14], where the strategy is to give up controlling the vehicle's yaw angle, and use the remaining propellers to achieve a horizontal spin.

This paper presents periodic solutions for a quadrocopter experiencing one, two opposing, or three complete rotor failures. The strategy employed is to define an axis, fixed with respect to the vehicle body, and have the vehicle rotate freely about this axis. By tilting this axis, and varying the total amount of thrust produced, the vehicle's position can be controlled. A linear, time invariant description of the attitude is used, allowing for straight-forward analysis of the system's controllability characteristics, and for controller synthesis.

The control strategy presented here for a single failed propeller is broadly similar to that of [14] in that the vehicle rotates freely about an axis, but differs in that the designer has an additional degree of freedom, to choose a ratio of the forces produced in equilibrium.

The methods presented in this paper could also be applied to design novel, rotating body vehicles. Such vehicles could be designed using as few as one propeller, and would thus be cheaper to produce than a quadrocopter, at the cost of not being able to control the full vehicle attitude. When equipped with a camera, such a vehicle could be used as a low-cost omnidirectional flying camera, similar to e.g. [15] or [16] .

This paper is organised as follows: Section II presents the equations governing the quadrocopter dynamics. Section III then presents periodic solutions to the equations of motion for the three different loss cases, while Section IV investigates under which conditions the system is controllable about these solutions. These results are then validated in Section V, and the paper concludes with an outlook in Section VI.

II. Equations of motion

The equations governing the motion of a quadrocopter are derived in this section. First, the translational and rotational dynamics are presented, followed by some simplifications for the sake of tractability. The kinematics of the reduced attitude, which is used later to describe the equilibria of the system and to design the controllers, are presented next. Boldface symbols like $\boldsymbol{g}$ are used throughout this paper to denote three-dimensional vectors, while non-boldface symbols like m will generally be used for scalars, with exceptions made explicit. The short-hand notation $\boldsymbol{\omega}^B = (p, q, r)$ will be used to denote the elements p, q, and r of the vector $\boldsymbol{\omega}^B$.

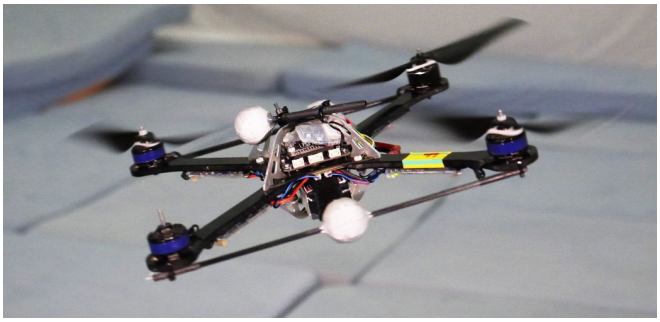

Fig. 1. A quadrocopter in controlled flight despite having lost one complete propeller.

The authors are with the Institute for Dynamic Systems and Control, ETH Zurich, Sonneggstrasse 3, 8092 Zurich, Switzerland.
{mullerm, rdandrea}@ethz.ch

978-1-4799-3684-7/14/$31.00 ©2014 IEEE

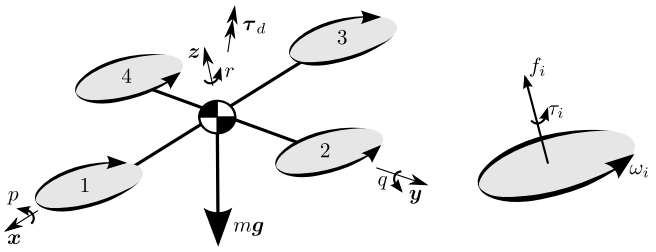

(A) (B)

Fig. 2. (A) A dynamic model of a quadrocopter with four propellers arranged symmetrically about the vehicle centre of mass, showing a body-fixed reference frame consisting of the directions $\boldsymbol{x}$, $\boldsymbol{y}$ and $\boldsymbol{z}$. Propellers 1 and 3 rotate in the opposite sense of propellers 2 and 4. A drag torque $\boldsymbol{\tau}_d$ acts to oppose the vehicle's angular velocity $\boldsymbol{\omega}^B$ expressed in the body-fixed frame as $\boldsymbol{\omega}^B = (p, q, r)$. The vehicle has a weight force $m\boldsymbol{g}$. (B) shows a detail of a propeller i rotating at angular velocity ω_i with respect to the body. Each propeller produces a thrust force f_i and torque τ_i, both in the direction of the propeller's axis of rotation. As drawn in (B), $\omega_i > 0$, and $\tau_i < 0$.

A. Dynamics

Fig. 2 shows a quadrocopter, with four propellers, and a total mass m. Five forces act on the vehicle: the weight $m\boldsymbol{g}$, and the four propeller forces of magnitude f_i which act in the body-fixed direction $\boldsymbol{z} = (0, 0, 1)$ as defined in the figure. Additionally, five torques act on the vehicle: one for each propeller (captured by the scalar τ_i) and a drag torque $\boldsymbol{\tau}_d$. The propeller torques oppose the propellers' rotation, and the vehicle drag torque $\boldsymbol{\tau}_d$ opposes the vehicle's angular velocity. Expressed in a body-fixed reference frame, the vehicle's angular velocity is $\boldsymbol{\omega}^B = (p, q, r)$. The rotation of the body-fixed frame with respect to some inertial frame is described by the rotation matrix $\mathbf{R}$.

The position of the quadrocopter's centre of mass, expressed in the inertial frame, is denoted $\boldsymbol{d} = (d_1, d_2, d_3)$. Then, the quadrocopter's translational dynamics are:

$$m\ddot{\boldsymbol{d}} = \mathbf{R}\boldsymbol{z}\sum_{i=1}^{4} f_i + m\boldsymbol{g} \tag{1}$$

with $\boldsymbol{g} = (0, 0, -9.81)\,\mathrm{m\,s^{-2}}$ the acceleration due to gravity.

The vehicle is assumed to consist of five rigid bodies: the vehicle body as such, and the four propellers (which are taken to include any rotating part of the motors). The vehicle body inertia tensor $\boldsymbol{I}^B$ is assumed to be diagonal when expressed in the body-fixed frame:

$$\boldsymbol{I}^B = \begin{bmatrix} I^B_{xx} & 0 & 0 \\ 0 & I^B_{yy} & 0 \\ 0 & 0 & I^B_{zz} \end{bmatrix}. \tag{2}$$

It is assumed that each propeller can be treated as a disk that is symmetric about its axis of rotation. This means that the propeller's rotational inertia expressed in the quadrocopter-fixed frame is independent of the orientation of the propeller, and equals

$$\boldsymbol{I}^P = \begin{bmatrix} I^P_{xx} & 0 & 0 \\ 0 & I^P_{xx} & 0 \\ 0 & 0 & I^P_{zz} \end{bmatrix}. \tag{3}$$

The differential equation governing the evolution of the body's angular velocity is now [17]

$$\begin{aligned} \boldsymbol{I}^B\dot{\boldsymbol{\omega}}^B + \sum_{i=1}^{4} \boldsymbol{I}^P\dot{\boldsymbol{\omega}}^{P_i} + \\ [\![\boldsymbol{\omega}^B\times]\!]\left(\boldsymbol{I}^B\boldsymbol{\omega}^B + \sum_{i=1}^{4}\boldsymbol{I}^P\left(\boldsymbol{\omega}^B + \boldsymbol{\omega}^{P_i}\right)\right) = \boldsymbol{\tau}_{\text{res}} \end{aligned} \tag{4}$$

with $\boldsymbol{\tau}_{\text{res}}$ the resultant torque acting on the body. The first two terms are the time derivative of the body rates and propeller speeds, respectively, and evaluate to

$$\boldsymbol{I}^B\dot{\boldsymbol{\omega}}^B = \left(I^B_{xx}\dot{p}, I^B_{yy}\dot{q}, I^B_{zz}\dot{r}\right) \tag{5}$$

$$\boldsymbol{I}^P\dot{\boldsymbol{\omega}}^{P_i} = \left(0, 0, I^P_{zz}\dot{\omega}_i\right). \tag{6}$$

The second term of (4) expresses the cross-coupling of the angular momentum in the system, due to taking the derivative in a non-inertial frame. Multiplying out the term yields

$$\begin{aligned} [\![\boldsymbol{\omega}^B\times]\!]\left(\boldsymbol{I}^B\boldsymbol{\omega}^B + \sum_{i=1}^{4}\boldsymbol{I}^P\left(\boldsymbol{\omega}^B + \boldsymbol{\omega}^{P_i}\right)\right) = \\ \begin{bmatrix} \left(I^T_{zz} - I^T_{yy}\right)qr + I^P_{zz}q\omega_\Sigma \\ -\left(I^T_{zz} - I^T_{xx}\right)pr - I^P_{zz}p\omega_\Sigma \\ \left(I^T_{yy} - I^T_{xx}\right)pq \end{bmatrix} \end{aligned} \tag{7}$$

having introduced the total inertias $I^T_{xx} = I^B_{xx} + 4I^P_{xx}$, $I^T_{yy} = I^B_{yy} + 4I^P_{xx}$, $I^T_{zz} = I^B_{zz} + 4I^P_{zz}$, and the sum of motor speeds $\omega_\Sigma = \omega_1 + \omega_2 + \omega_3 + \omega_4$.

$\boldsymbol{\tau}_{\text{res}}$, on the right hand side of (4), represents all the moments acting upon the body, which consist of the torques produced by the motors, and the moments due to the rotor forces. The centre of each rotor, through which the forces are assumed to act, is taken to lie at distance l from the centre of mass, such that

$$\boldsymbol{\tau}_{\text{res}} = \begin{bmatrix} (f_2 - f_4)\,l + \tau_{d_x} \\ (f_3 - f_1)\,l + \tau_{d_y} \\ \tau_1 + \tau_2 + \tau_3 + \tau_4 + \tau_{d_z} \end{bmatrix} \tag{8}$$

with $\boldsymbol{\tau}_d = \left(\tau_{d_x}, \tau_{d_y}, \tau_{d_z}\right)$ the components of the drag torque.

B. Further simplifying assumptions

There is a strong linear relationship between a propeller's reaction torque and thrust force (characterised by the coefficient κ_τ with the sign given by the sense of rotation). The thrust force of a stationary propeller is proportional to the angular velocity squared with coefficient κ_f, such that [18]

$$\tau_i = (-1)^{i+1}\kappa_\tau f_i \tag{9}$$

$$f_i = \kappa_f\omega_i^2. \tag{10}$$

For simplicity, the aerodynamic drag acting on the quadrocopter is assumed to act only to oppose the yaw rate r, with proportionality constant $\gamma > 0$ such that

$$\boldsymbol{\tau}_d = (0, 0, -\gamma r) \tag{11}$$

with the assumption of a linear drag term supported by experimental data. The fact that a term linear in the speed dominates, instead of a quadratic term, can possibly be

explained by the asymmetric relative air velocity over the advancing and retreating propeller blades (an effect exploited in a different context in [19]).

It is assumed that the propeller speeds are controlled by high bandwidth motors, such that the motor speed is unaffected by the vehicle motion. Furthermore, it is assumed that $\boldsymbol{I}^P \ll \boldsymbol{I}^B$, such that the term $\boldsymbol{I}^P\dot{\boldsymbol{\omega}}$ can be neglected. Note that the angular momentum of the rotors might still be comparable to that of the body, such that the term $\boldsymbol{I}^P\boldsymbol{\omega}^{P_i}$ may not be negligible compared to $\boldsymbol{I}^B\boldsymbol{\omega}^B$. The quadrocopter body is assumed to be symmetric, such that $I^B_{xx} = I^B_{yy}$.

Expanding (4) with (2)-(3), (5)-(8) and applying the above assumptions yields the following three differential equations for the vehicle's body rates:

$$I^B_{xx}\dot{p} = \kappa_f\left(\omega_2^2 - \omega_4^2\right)l - \left(I^T_{zz} - I^T_{xx}\right)qr - I^P_{zz}q\left(\omega_1 + \omega_2 + \omega_3 + \omega_4\right), \tag{12}$$

$$I^B_{xx}\dot{q} = \kappa_f\left(\omega_3^2 - \omega_1^2\right)l + \left(I^T_{zz} - I^T_{xx}\right)pr + I^P_{zz}p\left(\omega_1 + \omega_2 + \omega_3 + \omega_4\right), \tag{13}$$

$$I^B_{zz}\dot{r} = -\gamma r + \kappa_\tau\kappa_f\left(\omega_1^2 - \omega_2^2 + \omega_3^2 - \omega_4^2\right). \tag{14}$$

C. Reduced attitude kinematics

A typical quadrocopter controller (see e.g. [20]) allows for control of the quadrocopter's full attitude $\mathbf{R}$ to some desired attitude as part of the control strategy. The strategy adopted herein is to give up control of the full attitude once a propeller has failed, and instead control only a single direction of the attitude (or, the attitude to within one degree of freedom), often referred to as a reduced attitude [21], which can be described by a unit vector.

The differential equation governing the evolution of a unit vector stationary in the inertial frame but expressed in the body-fixed frame as $\boldsymbol{n} = (n_x, n_y, n_z)$ is given by the cross product

$$\dot{\boldsymbol{n}} = -\boldsymbol{\omega}^B \times \boldsymbol{n}. \tag{15}$$

III. Periodic solutions and equilibria

This section presents periodic solutions for the position and attitude of a quadrocopter experiencing the loss of one, two (opposing) or three propellers. For the case of one and three lost propellers, the resultant forces and torques acting on the vehicle will not be zero, such that no static equilibrium exists for the vehicle's centre of mass. However, in each case the reduced attitude of the vehicle is constant, such that the controllability of the system's attitude can be investigated with methods well-established for linear, time-invariant, systems in Section IV. An overbar will be used to express values constant along the periodic solution (e.g. $\bar{p}$).

The goal is to find periodic solutions in which a constant primary axis $\bar{\boldsymbol{n}}$ exists about which the vehicle rotates with constant angular velocity $\bar{\boldsymbol{\omega}}^B$. The primary axis is fixed with respect to the vehicle body, and is expressed in the body fixed frame as $\bar{\boldsymbol{n}} = (\bar{n}_x, \bar{n}_y, \bar{n}_z)$. From (15), the requirement that $\dot{\bar{\boldsymbol{n}}} = 0$, and the properties of the cross product, it follows that

$$\bar{\boldsymbol{n}} = \epsilon\,\bar{\boldsymbol{\omega}}^B \tag{16}$$

with the norm constraint on $\boldsymbol{n}$ expressed by

$$\|\bar{\boldsymbol{n}}\| = \left\|\epsilon\,\bar{\boldsymbol{\omega}}^B\right\| = 1 \tag{17}$$

where $\|\cdot\|$ is the Euclidean norm.

The primary axis is taken to point opposite to gravity along the periodic solution, and the vehicle is required to not accelerate in the direction of gravity. The fraction of the total thrust force $\bar{f}_\Sigma = \bar{f}_1 + \bar{f}_2 + \bar{f}_3 + \bar{f}_4$ pointing opposite to gravity is thus $\bar{n}_z$, such that

$$\bar{f}_\Sigma\,\bar{n}_z = m\,\|\boldsymbol{g}\|. \tag{18}$$

If $\bar{n}_z < 1$, a part of the total thrust force will point perpendicular to gravity, imparting an acceleration of the vehicle in this direction. In this case, the vehicle will move along a horizontal circular trajectory with a period of

$$T_{ps} = \frac{2\pi}{\|\bar{\boldsymbol{\omega}}^B\|} \tag{19}$$

and a radius of

$$\bar{R}_{ps} = \frac{\sqrt{1-\bar{n}_z^2}}{\bar{n}_z}\frac{\|\boldsymbol{g}\|}{\|\bar{\boldsymbol{\omega}}^B\|^2}. \tag{20}$$

The solutions will now be presented for each case of a quadrocopter losing one propeller, two opposing propellers, and three propellers. This involves solving for the eleven unknowns $\bar{n}_x$, $\bar{n}_y$, $\bar{n}_z$, $\bar{p}$, $\bar{q}$, $\bar{r}$, ϵ, $\bar{\omega}_1$, $\bar{\omega}_2$, $\bar{\omega}_3$ and $\bar{\omega}_4$ by utilising the eight algebraic equations (12) - (14) (with the angular accelerations set to zero) and (16) - (18).

The symmetry properties of the quadrocopter mean that the equilibrium yaw rate is independent of the pitch and roll rates from (14), and can be solved independently as

$$\bar{r} = \frac{\kappa_\tau\kappa_f}{\gamma}\left(\bar{\omega}_1^2 - \bar{\omega}_2^2 + \bar{\omega}_3^2 - \bar{\omega}_4^2\right). \tag{21}$$

Each lost motor/propeller will add a constraint of the form $\omega_i = 0$, and the solutions for each of the loss cases will be considered in more detail below.

A. Solution with one lost propeller

Without loss of generality it will be assumed that propeller 4 has failed, such that $f_4 = \tau_4 = 0$, and specifically that $\bar{\omega}_4 = 0$, leaving two degrees of freedom for solving for the periodic solution. An intuitive way of specifying them is for the two opposing propellers to produce equal thrust (thus $\bar{f}_1 = \bar{f}_3$), and choosing a ratio $\rho = \bar{f}_2/\bar{f}_1$ between the thrust of propellers 1 and 2, such that ρ becomes a tuning factor. This leaves eleven nonlinear equations to solve for eleven unknowns.

From (13), one solution is $\bar{p} = 0$ and thus $\bar{n}_x = 0$, for all choices of ρ. For small ρ, as ρ grows, $\bar{n}_z$ decreases and thus the total force required increases by (18). The radius $\bar{R}_{ps}$ of the horizontal orbit (20) will be zero at $\rho = 0$, but the relationship between the angular velocity and ρ is harder to predict, and numerical results are given for a specific quadrocopter in Section V, specifically Fig. 3. Note that for $\rho = 0$ the two-propeller solution of Section III-B, below, is recovered, while as ρ tends to infinity the single propeller solution of Section III-A is recovered (with instead propellers 1, 3 and 4 taken as failed).

B. Solution with two lost propellers

It is assumed that two opposing propellers have failed, taken without loss of generality to be 2 and 4. Note that the case of two adjacent propellers failing will not be addressed here, and is a topic to be investigated in future work.

Setting $\bar{\omega}_2 = \bar{\omega}_4 = 0$ leaves one degree of freedom, which can be resolved by requiring that the remaining motors produce equal thrust, i.e. $\bar{\omega}_1 = \bar{\omega}_3$. The equilibrium can now be solved for as follows:

$$\bar{f}_1 = \bar{f}_3 = \frac{1}{2} m \|\boldsymbol{g}\| \tag{22}$$

$$\bar{\omega}_1 = \bar{\omega}_3 = -\sqrt{\frac{m\|\boldsymbol{g}\|}{2\kappa_f}} \tag{23}$$

$$\bar{\boldsymbol{\omega}}^B = \left(0, 0, \frac{\kappa_\tau m \|\boldsymbol{g}\|}{\gamma}\right) \tag{24}$$

$$\bar{\boldsymbol{n}} = (0, 0, 1)\,. \tag{25}$$

For the two-propeller case, $\bar{R}_{ps} = 0$ and the vehicle will be stationary at a point in space with its $\boldsymbol{z}$ axis pointing vertically.

C. Solution with three lost propellers

Propellers 2, 3 and 4 are taken to have failed, again without loss of generality, such that the system is fully constrained. From (12) follows that one solution is for $\bar{q} = \bar{n}_y = 0$, and then $\bar{p} \neq 0$ and thus $\bar{n}_x \neq 0$. The solution for a specific vehicle is given in Section V.

IV. Controllability

It is shown below that the vehicle's reduced attitude is controllable near the equilibrium solutions of the preceding section. This is done by exploiting the time invariant nature of the attitude equilbria and linearising about them, and examining the rank of the controllability matrix [22]. The state vector $s = (p, q, n_x, n_y)$ is introduced to describe the vehicle's reduced attitude, and the conditions under which this reduced attitude is controllable are derived below for the three different propeller loss cases discussed in this paper. The actual design and implementation of a controller for a specific vehicle is deferred until Section V. Given that the total vehicle thrust can be specified, and that simultaneously the direction of the vehicle's thrust can be controlled, the vehicle's acceleration can be controlled (at least quasi-statically) and thus also its position.

The attitude deviation from the equilibrium is written as $\tilde{s} = s - \bar{s}$, and will evolve to first order as

$$\dot{\tilde{s}} = A\tilde{s} + Bu \tag{26}$$

$$A = \left.\frac{\partial \dot{s}}{\partial s}\right|_{s=\bar{s}} = \begin{bmatrix} 0 & \bar{a} & 0 & 0 \\ -\bar{a} & 0 & 0 & 0 \\ 0 & -\bar{n}_z & 0 & \bar{r} \\ \bar{n}_z & 0 & -\bar{r} & 0 \end{bmatrix} \tag{27}$$

defining the coupling constant $\bar{a}$ as

$$\bar{a} = \frac{I^T_{xx} - I^T_{zz}}{I^B_{xx}} \bar{r} - \frac{I^P_{zz}}{I^B_{xx}} \left(\bar{\omega}_1 + \bar{\omega}_2 + \bar{\omega}_3 + \bar{\omega}_4\right) \tag{28}$$

and introducing an input u, which enters the system through the matrix B. The definition of B and u will be deferred to the sections below, depending on the number of remaining propellers.

A. Control with one lost propeller

With three propellers remaining, the input vector $u = (u_1, u_2)$ is introduced as a function of the deviations of the actual motor forces from the equilibrium, with units of force

$$u_1 = \left(f_3 - \bar{f}_3\right) - \left(f_1 - \bar{f}_1\right) \tag{29}$$

$$u_2 = \left(f_2 - \bar{f}_2\right). \tag{30}$$

The remaining degree of freedom is resolved by specifying that the total thrust matches the desired thrust:

$$f_1 + f_2 + f_3 = \bar{f}_1 + \bar{f}_2 + \bar{f}_3. \tag{31}$$

The system (26) is expanded to include these inputs as

$$\dot{\tilde{s}} = A\tilde{s} + B_{(3)}u \tag{32}$$

$$B_{(3)} = \frac{l}{I^B_{xx}} \begin{bmatrix} 0 & 1 \\ 1 & 0 \\ 0 & 0 \\ 0 & 0 \end{bmatrix}. \tag{33}$$

Examining the rank of the controllability matrix $\mathcal{C}_{(3)} = \begin{bmatrix} B_{(3)} & AB_{(3)} & A^2B_{(3)} & A^3B_{(3)} \end{bmatrix}$ it is easy to show that (32) is controllable if $l \neq 0$ and $\bar{n}_z \neq 0$.

B. Control with two lost propellers

Having lost two opposing propellers, the system has a single input u_1, defined as in (29), which is now added to (26) to give

$$\dot{\tilde{s}} = A\tilde{s} + B_{(2)}u \tag{34}$$

$$B_{(2)} = \frac{l}{I^B_{xx}} \begin{bmatrix} 0 \\ 1 \\ 0 \\ 0 \end{bmatrix}. \tag{35}$$

Again, the total thrust produced must match the commanded thrust

$$f_1 + f_3 = \bar{f}_1 + \bar{f}_3. \tag{36}$$

The two propeller system (34) is controllable if $\mathcal{C}_{(2)} = \begin{bmatrix} B_{(2)} & AB_{(2)} & A^2B_{(2)} & A^3B_{(2)} \end{bmatrix}$ has full rank, or equivalently if the determinant of $\mathcal{C}_{(2)}$ is non-zero, i.e.

$$\bar{a}\,\bar{r}\,\bar{n}_z^2 \left(\bar{a} + \bar{r}\right)^2 \left(\frac{l}{I^B_{xx}}\right)^4 \neq 0. \tag{37}$$

Combining this with (24), and assuming $l \neq 0$ this leaves

$$\bar{a}\,\bar{n}_z^2 \left(\bar{a} + \bar{r}\right)^2 \neq 0. \tag{38}$$

Note that for the two-propeller case, by (25), $n_z = 1$. Thus the system is uncontrollable if $\bar{a} = 0$, or

$$\left(I^T_{xx} - I^T_{zz}\right)\bar{r} = 2I^P_{zz}\bar{\omega}_1 \tag{39}$$

in which case the vehicle roll rate p is uncontrollable.

If instead $\bar{a} + \bar{r} = 0$, or

$$\left(I_{xx}^T + I_{xx}^B - I_{zz}^T\right)\bar{r} = 2I_{zz}^P\bar{\omega}_1 \tag{40}$$

the linearised system has two uncontrollable modes corresponding to $p + \bar{a}n_x$ and n_y.

C. Control with three lost propellers

The description of the linearised attitude system when using only a single propeller is the same as that for two propellers (see Section IV-B) except that now $f_3 = 0$ and $\omega_3 = 0$. The controllability requirement is then the same as (37). Noting that $\bar{n}_z = 0$ is not a physically meaningful possibility as the total force given by (18) would then be undefined, the linearised quadrocopter attitude is not controllable with a single propeller if either of the two below equalities hold:

$$\left(I_{zz}^T - I_{xx}^T\right)\bar{r} = I_{zz}^P\bar{\omega}_1 \tag{41}$$

$$\left(I_{zz}^T - I_{xx}^T - I_{xx}^B\right)\bar{r} = I_{zz}^P\bar{\omega}_1. \tag{42}$$

Note that in the one-propeller case the total thrust will vary with u_1 as this can not be specified as in (31) and (36).

V. Validation

The preceding analysis is validated in experiment and simulation in this section. A cascaded control design is implemented for each case of a quadrocopter losing one, two opposing, or three propellers, with a slow outer loop controlling the vehicle's position, and a fast inner loop controlling the reduced attitude. An LQR controller [23] is implemented in each case for the inner loop control.

A. Experimental platform

The work was validated using quadrocopters based on the Ascending Technologies Hummingbird [24], in the Flying Machine Arena [25], which will be referred to here simply as "the quadrocopter". The attitude controller of Section IV is executed at $1000\,\text{Hz}$ on board the vehicle, while the translational controller presented below is executed at $50\,\text{Hz}$.

The quadrocopter's inertia was measured by measuring its period of oscillation when suspended around three different axes, and was found to be $I_{xx}^T = 3.2 \times 10^{-3}\text{kg m}^2$, $I_{zz}^T = 5.5 \times 10^{-3}\text{kg m}^2$. The propeller inertia was estimated by approximating the propeller and motor rotor as disks and cylinders, respectively, to get $I_{zz}^P = 1.5 \times 10^{-5}\text{kg mm}^2$, while the other propeller inertia was neglected $I_{xx}^P = 0$. The vehicle's mass was measured to be $0.50\,\text{kg}$, and the distance from the centre of mass to the centre of the propellers is $l = 0.17\,\text{m}$.

The propellers used were characterised using a force-torque sensor, and the thrust and reaction torque coefficients were estimated as $\kappa_f = 6.41 \times 10^{-6}\text{Ns}^2\,/\text{rad}^2$ and $\kappa_\tau = 1.69 \times 10^{-2}\text{Nm/ N}$, respectively. The propellers are able to produce thrust forces in the range

$$f_i \in [0.2, 3.8]\,\text{N}. \tag{43}$$

The quadrocopter's drag coefficient was estimated to be $\gamma = 2.75 \times 10^{-3}\text{N m s rad}^{-1}$.

B. Translational controller

When using fewer than four propellers, only the direction of the primary axis $\boldsymbol{n}$ is controlled, in contrast to the nominal quadrocopter case where the full attitude $\mathbf{R}$ is controlled. The direction of the primary axis, and the total thrust that the vehicle produces, affect the vehicle acceleration through (1). A cascaded control strategy is designed, with a fast inner loop controlling the vehicle's reduced attitude, and a slow outer loop controlling the vehicle's position.

The translational deviation of the quadrocopter from a desired point in space is written as $\boldsymbol{d}$. The goal of the translational controller is to make this deviation behave like a second-order system, with damping ratio ζ and natural frequency ω_n, by introducing the desired acceleration $\ddot{\boldsymbol{d}}_{des}$ such that

$$\ddot{\boldsymbol{d}}_{des} + 2\zeta\omega_n\dot{\boldsymbol{d}} + \omega_n^2\boldsymbol{d} = 0. \tag{44}$$

The damping ratio was set to $\zeta = 0.7$, and ω_n was chosen for each of the cases such that the translational system responds much slower than the attitude system. The direction of the instantaneously desired direction of the primary axis $\boldsymbol{n}_{des}$, and the total thrust produced f_Σ, are defined as

$$\boldsymbol{n}_{des}\bar{n}_z f_\Sigma = m\mathbf{R}^{-1}\left(\ddot{\boldsymbol{d}}_{des} - \boldsymbol{g}\right) \tag{45}$$

$$f_\Sigma = f_1 + f_2 + f_3 + f_4. \tag{46}$$

This can be easily adapted, so that the horizontal and vertical degrees of freedom have different natural frequencies/damping ratios.

The fast inner controller, as described in Section IV, must then make the vehicle's primary axis align with $\boldsymbol{n}_{des}$ while producing a total thrust f_Σ. Note that for $\ddot{\boldsymbol{d}}_{des} = 0$, the solutions of Section III are recovered.

C. Motor time constants

It was found in experiment that the motor dynamics have a large influence on the system behaviour. For this reason, the reduced attitude system (26) of Section IV was extended as follows. The currently produced force deviations were added as states, each tracking its respective command as a first order system with time constant σ_{mot}. Thus the linearised system for i propellers now becomes

$$\dot{s}_e = A_e s_e + B_{(i)e}u_e \tag{47}$$

$$A_e = \begin{bmatrix} A & B_{(i)} \\ \mathbf{0} & -\sigma_{mot}^{-1}\mathbf{1} \end{bmatrix} \tag{48}$$

$$B_e = \begin{bmatrix} \mathbf{0} \\ \sigma_{mot}^{-1}\mathbf{1} \end{bmatrix} \tag{49}$$

with $\mathbf{0}$ and $\mathbf{1}$ being zero and identity matrices of the appropriate dimension, respectively.

The time constant for the quadrocopter was estimated to be $\sigma_{mot} = 0.015\,\text{s}$.

D. Implementation for one lost propeller

The equilibrium for the quadrocopter with three propellers for different values of $\rho = \bar{f}_2/\bar{f}_1$ is investigated in Fig. 3. The absolute body rate has a minimum of

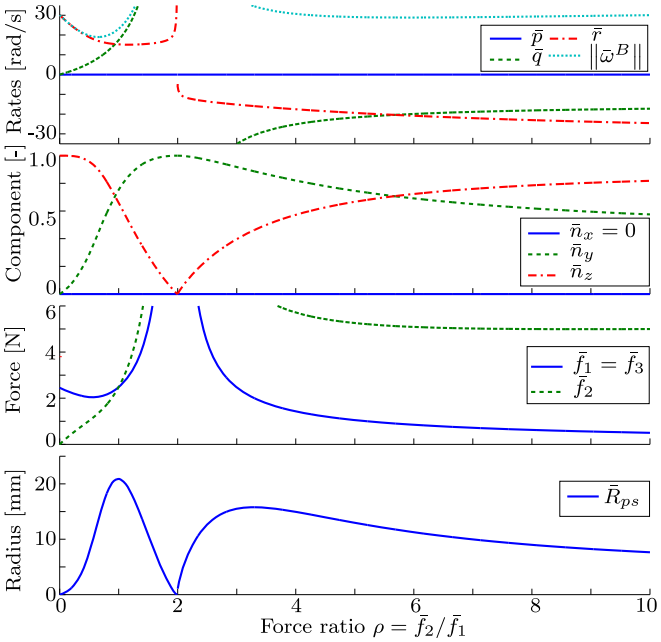

Fig. 3. The equilibrium state for the quadrocopter when using three propellers, as a function of the ratio $\rho = \bar{f}_2/\bar{f}_1$, showing from top to bottom the angular velocity, the direction of the primary axis, the thrust forces and the radius of the horizontal motion. Note that by design $\bar{f}_3 = \bar{f}_1$. As the force $\bar{f}_2$ increases, it can be seen that the primary axis $\bar{\boldsymbol{n}}$ of the vehicle initially moves farther away from the body $\boldsymbol{z}$ axis, while the resultant pitch rate $\bar{q}$ increases. Note the discontinuity at $\rho = 2$, when $\bar{r} = \bar{n}_z = 0$, and after which the sense of rotation reverses. At $\rho = 0$ the solution is that of the two-propeller case, while for large ρ the solution approaches that of the single propeller case.

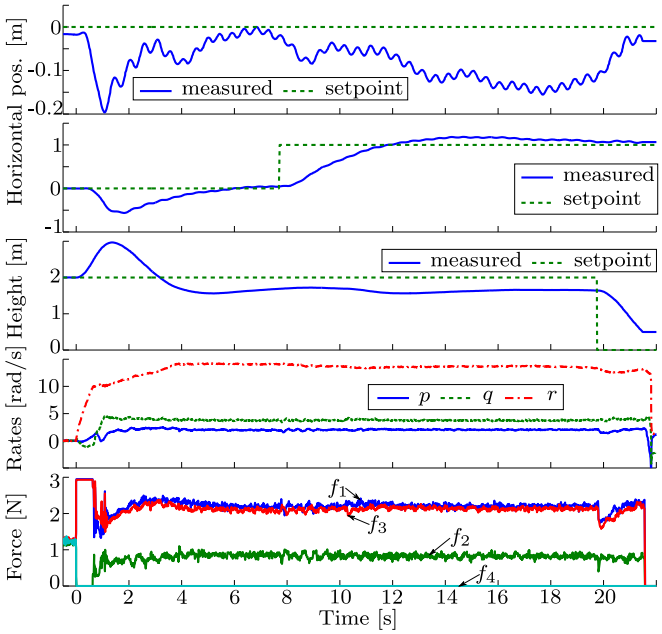

Fig. 4. Experimental results for a quadrocopter at hover, with propeller 4 disabled at time 0. The first three plots show the two horizontal directions, and the vertical. The desired position setpoint is shifted hoizontally by 1 m after 7.7 s, and the height setpoint is set to zero after 19.8 s, and the vehicle lands at 21.5 s. Initially, the vehicle only uses two opposing propellers to build up angular momentum, and the controller is enabled when the vehicle angular velocity exceeds $10\,\mathrm{rad\,s^{-1}}$ (at 0.62 s). The oscillatory motion of the vehicle about the setpoint can be seen clearly on the top plot.

$\|\bar{\boldsymbol{\omega}}^B\| = 19.0\,\mathrm{rad\,s^{-1}}$ at $\rho = 0.655$, while the propeller force $\bar{f}_1$ has a minimum in the region $\rho \in [0, 2]$ of $\bar{f}_1 = 2.04\,\mathrm{N}$ at $\rho = 0.563$, with both minima being shallow. A value of $\rho = 0.5$ was chosen for the implementation, placing all steady-state thrust forces some distance away from the saturation values (43). In this case, the attitude equilibrium values are

$$\bar{f}_1 = \bar{f}_3 = 2.05\,\mathrm{N},\ \bar{f}_3 = 1.02\,\mathrm{N} \tag{50}$$
$$\bar{\boldsymbol{\omega}}^B = (0, 5.69, 18.89)\,\mathrm{rad\,s^{-1}} \tag{51}$$
$$\bar{\boldsymbol{n}} = (0, 0.289, 0.958) \tag{52}$$
$$\bar{R}_{ps} = 8\,\mathrm{mm}. \tag{53}$$

An LQR controller was designed on the extended system, with a diagonal state and input cost matrices, with the cost value of $1\,\mathrm{s^2\ rad^{-2}}$ on the angular rates, 20 on the deviation from the primary axis, zero on the extended motor states, and $1\,\mathrm{N^{-2}}$ on the inputs. The translational controller natural frequency was set to $\omega_n = 1\,\mathrm{rad\,s^{-1}}$.

The resulting controller was implemented on the system, and results are shown in Fig. 4 for a quadrocopter starting at hover at a height of 2 m. At time 0, the fourth propeller is disabled, and the vehicle initially uses only the two opposing propellers to produce an angular velocity about the $\boldsymbol{z}$ axis. Once this angular velocity exceeds $10\,\mathrm{rad\,s^{-1}}$, the LQR controller is used to control the vehicle (at 0.62 s). The control strategy stabilises the vehicle around the desired position, also when the position is shifted 1 m horizontally, and also allows the vehicle to perform a soft landing.

When maintaining a position, the vehicle's state is approximately as below:

$$f_1 = 2.2\,\mathrm{N},\ f_2 = 2.1\,\mathrm{N},\ f_3 = 0.8\,\mathrm{N} \tag{54}$$
$$\boldsymbol{\omega}^B = (2.1, 3.7, 13.7)\,\mathrm{rad\,s^{-1}} \tag{55}$$
$$\boldsymbol{n} = (0.14, 0.26, 0.96)\,. \tag{56}$$

Fig. 1 shows a quadrocopter in flight with one lost propeller, and the video accompanying this paper shows a quadrocopter taking off despite the loss of one propeller, translating 2 m horizontally, and then landing.

E. Implementation for two lost propellers

The equilibrium condition for the quadrocopter flying with two opposing propellers with equal equilibrium thrusts is calculated by (22) - (25) as

$$\bar{f}_1 = \bar{f}_3 = 2.45\,\mathrm{N} \tag{57}$$
$$\bar{\omega}_1 = \bar{\omega}_3 = -619\,\mathrm{rad\,s^{-1}} \tag{58}$$
$$\bar{\boldsymbol{\omega}}^B = (0, 0, 30.1)\,\mathrm{rad\,s^{-1}} \tag{59}$$

Again, an LQR controller was designed on the extended two-propeller system, with a diagonal state and input cost matrices, with the cost value of 0 on the angular rates, 1000 on the deviation from the primary axis along $\boldsymbol{x}$, 2 on the deviation from the primary axis along $\boldsymbol{y}$, zero on the extended motor states, and $0.75\,\mathrm{N^{-2}}$ on the inputs. The

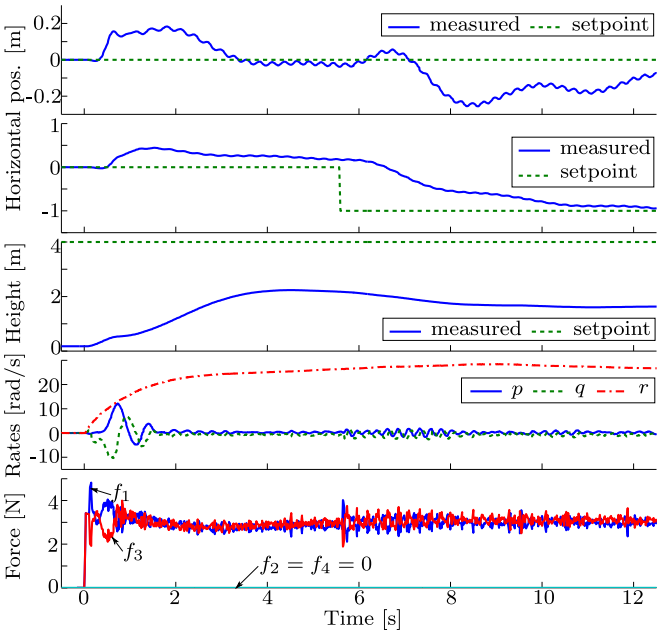

Fig. 5. Experimental results for a quadrocopter flying with only two propellers. The quadrocopters starts at rest, on the ground, at time zero. After 5.6 s the horizontal setpoint is shifted by 1 m. Note that the vehicle does not reach the desired height, and has a height error of approximately 2.4 m.

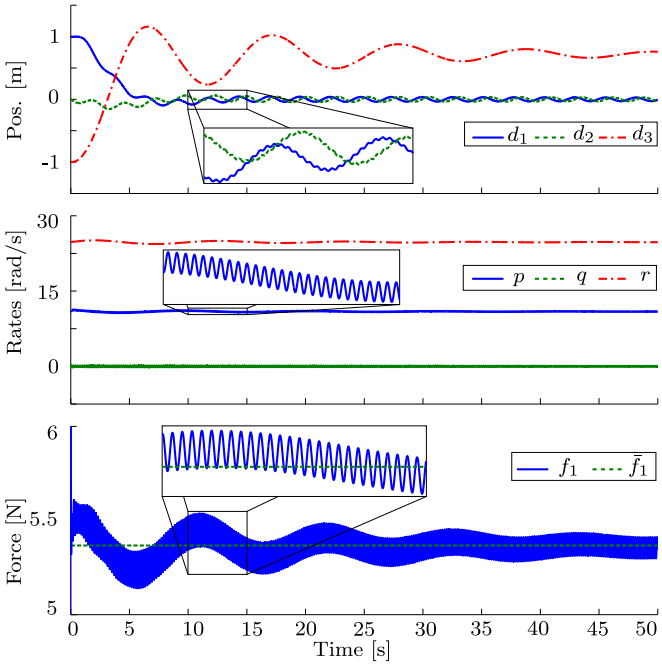

Fig. 6. Nonlinear simulation results for a quadrocopter flying with only one propeller. The simulation is started with the vehicle at the reduced attitude solution of Section III-C, but with a 1 m offset both in the horizontal and vertical directions. The controller successfully reduces the horizontal error, but a vertical offset of 0.75 m remains. Note that the maximum producible thrust in this simulation was set to double that of the true system.

translational controller was left as for the single propeller loss case: $\omega_n = 1\,\mathrm{rad\,s^{-1}}$.

The resulting controller was implemented on the system, and results are shown in Fig. 5 for a quadrocopter taking off from the ground with only two propellers. After 5.6 s, the horizontal setpoint is shifted by 1 m. Notable is that the vehicle has a large steady-state offset in the height, indicating that the propellers produce significantly less thrust than expected when the body is rotating at high angular velocities. In practise, this could be solved by implementing an integral controller on the vehicle height, or by more accurately modelling the behaviour of the propellers when rotating. When maintaining a position, the following states were measured:

$$f_1 = 2.98\,\mathrm{N},\ f_3 = 3.10\,\mathrm{N} \tag{60}$$

$$\boldsymbol{\omega}^B = (0.22, -0.72, 27.1)\,\mathrm{rad\,s^{-1}}. \tag{61}$$

A quadrocopter taking off with two propellers, translating two metres horizontally, and then landing can be seen in the accompanying video.

F. Implementation for three lost propellers

When utilising only a single propeller, the equilibrium condition was calculated as

$$\bar{f}_1 = 5.37\,\mathrm{N},\ \bar{\omega}_1 = -915\,\mathrm{rad\,s^{-1}} \tag{62}$$

$$\bar{\boldsymbol{\omega}}^B = (14.7, 0, 33.0)\,\mathrm{rad\,s^{-1}} \tag{63}$$

$$\bar{\boldsymbol{n}} = (0.41, 0, 0.91)\,. \tag{64}$$

Because the required force $\bar{f}_1$ exceeds the thrust limits (43) this equilibrium could not be implemented on the quadrocopter. Furthermore, when starting from a hover, a vehicle losing propellers 2, 3 and 4 will have a much stronger tendency to accelerate about the $\boldsymbol{y}$ axis than the $\boldsymbol{z}$ axis (because $l \gg \kappa_\tau$). This implies that it is non-trivial to bring a vehicle from a stationary state to a state sufficiently close to equilibrium for a linear control strategy to be effective.

A nonlinear simulation was used to validate the single propeller case. The simulator implemented the dynamic equations of Section II with the properties of the quadrocopters as given above, except that the maximum thrust force limit was doubled to 7.6 N. In the simulation, the simulated motor speeds track the commanded speeds as first order systems with time constant 0.015 s.

The LQR controller was designed with a cost of $1\,\mathrm{s^2 rad^{-2}}$ on the angular rates, 100 on the attitude deviations, zero on the extended motor state, and $4\,\mathrm{N^{-2}}$ on the input. The translational controller was parametrised with $\omega_n = 0.5\,\mathrm{rad\,s^{-1}}$.

The simulation was started with the vehicle's attitude at the periodic solution, but with a 1 m horizontal error, and a 1 m vertical error. The results are shown in Fig. 6 – the vehicle is brought to the correct horizontal position, but the vehicle height shows a steady state offset of approximately 0.75 m.

G. Discussion

The implemented two-propeller solution uses only slightly more thrust per propeller than the three propeller solution, but has significantly less total thrust at the periodic solution (due to using only two propellers, and having $\bar{n}_z = 1$) and

could thus be expected to be more energy efficient. However, the three propeller case has two independent inputs on the attitude system compared to one independent input for the two-propeller case – the attached video shows a close-up of the two cases, and it can be clearly seen that the three-propeller solution remains closer to the setpoint than the two-propeller solution. This effect can also be seen when comparing Fig. 4 and Fig. 5. A future topic of research will be to quantify the sensitivity of the system to noise for different values of ρ.

VI. Outlook

This paper presents equilibrium states and controllers that allow a quadrocopter to maintain a position in space after losing one, two (opposing), or three propellers. The strategy in each case is to have the vehicle rotate freely about an axis, fixed with respect to the body. The remaining motor forces are then used to rotate this axis in inertial space, which allows the vehicle to translate in space when combined with the total thrust produced. A cascaded control scheme exploiting time scale separation was used to control the translation. The strategy is implemented and validated with data gathered by experiment for the cases of losing a single and two opposing propellers, while the case of losing three propellers was validated in a nonlinear simulation.

In future work, the authors intend to more accurately characterise the vehicle, specifically the aerodynamic effects affecting the propellers, and to construct a flying single propeller vehicle. The authors also intend to implement the presented results with a fault detection scheme, and investigate different switching strategies for transitioning from e.g. four propellers to three.

Acknowledgements

The Flying Machine Arena is the result of contributions of many people, a full list of which can be found at `http://www.idsc.ethz.ch/Research_DAndrea/FMA/participants`. The authors thank Raymond Oung for making available the propeller characterisation data.

This research was supported by the Swiss National Science Foundation through grant agreement number 138112.

References

[1] F. Fraundorfer, L. Heng, D. Honegger, G. H. Lee, L. Meier, P. Tanskanen, and M. Pollefeys, "Vision-based autonomous mapping and exploration using a quadrotor MAV," in *IEEE/RSJ International Conference on Intelligent Robots and Systems*. IEEE, 2012, pp. 4557–4564.

[2] S. Weiss, M. W. Achtelik, S. Lynen, M. C. Achtelik, L. Kneip, M. Chli, and R. Siegwart, "Monocular vision for long-term micro aerial vehicle state estimation: A compendium," *Journal of Field Robotics*, vol. 30, no. 5, pp. 803–831, 2013.

[3] W. Selby, P. Corke, and D. Rus, "Autonomous aerial navigation and tracking of marine animals," in *Proceedings of the 2011 Australasian Conference on Robotics and Automation*. Australian Robotics & Automation Association, 2011, pp. 1–7.

[4] J. Rasmussen, J. Nielsen, F. Garcia-Ruiz, S. Christensen, and J. C. Streibig, "Potential uses of small unmanned aircraft systems (UAS) in weed research," *Weed Research*, 2013.

[5] J. Fink, N. Michael, S. Kim, and V. Kumar, "Planning and control for cooperative manipulation and transportation with aerial robots," *The International Journal of Robotics Research*, vol. 30, no. 3, pp. 324–334, 2011.

[6] J. R. Horandel, S. Buitink, A. Corstanje, J. E. Enriquez, and H. Falcke, "The LOFAR radio telescope as a cosmic ray detector," in *International Cosmic Ray Conference*, 2013.

[7] D. Scaramuzza, M. Achtelik, L. Doitsidis, F. Fraundorfer, E. Kosmatopoulos, A. Martinelli, M. Achtelik, M. Chli, S. Chatzichristofis, L. Kneip *et al.* (2013) Vision-controlled micro flying robots: from system design to autonomous navigation and mapping in gps-denied environments. [online] http://robotics.ethz.ch/~scaramuzza/Davide_Scaramuzza_files/publications/pdf/IEEE_RAM_submitted.pdf.

[8] A. Marks, J. F. Whidborne, and I. Yamamoto, "Control allocation for fault tolerant control of a VTOL octorotor," in *UKACC International Conference on Control*. IEEE, 2012, pp. 357–362.

[9] Y. Zhang, A. Chamseddine, C. Rabbath, B. Gordon, C.-Y. Su, S. Rakheja, C. Fulford, J. Apkarian, and P. Gosselin, "Development of advanced FDD and FTC, techniques with application to an unmanned quadrotor helicopter testbed," *Journal of the Franklin Institute*, 2013.

[10] (2013, September) Multicopter, quadcopter, drone, RC aircraft recovery and rescue chutes. [online] http://www.fruitychutes.com/uav_rpv_drone_recovery_parachutes/multicopter_quadcopter-rc_aircraft_recovery_and_rescue_chutes.htm.

[11] M. Ranjbaran and K. Khorasani, "Fault recovery of an under-actuated quadrotor aerial vehicle," in *IEEE Conference on Decision and Control*. IEEE, 2010, pp. 4385–4392.

[12] H. A. Izadi, Y. Zhang, and B. W. Gordon, "Fault tolerant model predictive control of quad-rotor helicopters with actuator fault estimation," in *IFAC World Congress*, vol. 18, no. 1, 2011, pp. 6343–6348.

[13] A. Chamseddine, Y. Zhang, C. A. Rabbath, C. Join, and D. Theilliol, "Flatness-based trajectory planning/replanning for a quadrotor unmanned aerial vehicle," *IEEE Transactions on Aerospace and Electronic Systems*, vol. 48, no. 4, pp. 2832–2848, 2012.

[14] A. Freddi, A. Lanzon, and S. Longhi, "A feedback linearization approach to fault tolerance in quadrotor vehicles," in *IFAC World Congress*, 2011, pp. 5413–5418.

[15] T. Haus, M. Orsag, and S. Bogdan, "Omnidirectional vision based surveillance with spincopter," in *International Conference on Unmanned Aircraft Systems*, 2013, pp. 326–332.

[16] H. Youngren, S. Jameson, and B. Satterfield, "Design of the samarai monowing rotorcraft nano air vehicle," in *Proceedings of the American Helicopter Society AHS 65th Annual Forum and Technology Display*, 2009.

[17] P. H. Zipfel, *Modeling and Simulation of Aerospace Vehicle Dynamics Second Edition*. AIAA, 2007.

[18] P. Pounds, R. Mahony, P. Hynes, and J. Roberts, "Design of a four-rotor aerial robot," in *Australasian Conference on Robotics and Automation*, vol. 27, 2002, p. 29.

[19] P. Martin and E. Salaün, "The true role of accelerometer feedback in quadrotor control," in *IEEE International Conference on Robotics and Automation*, 2010, pp. 1623–1629.

[20] R. Mahony, V. Kumar, and P. Corke, "Aerial vehicles: Modeling, estimation, and control of quadrotor," *IEEE robotics & automation magazine*, vol. 19, no. 3, pp. 20–32, 2012.

[21] N. A. Chaturvedi, A. K. Sanyal, and N. H. McClamroch, "Rigid-body attitude control," *Control Systems, IEEE*, vol. 31, no. 3, pp. 30–51, 2011.

[22] F. Callier and C. Desoer, *Linear System Theory*, ser. Springer Texts in Electrical Engineering. Springer, 1994.

[23] D. P. Bertsekas, *Dynamic Programming and Optimal Control, Vol. II*. Athena Scientific, 2007.

[24] D. Gurdan, J. Stumpf, M. Achtelik, K.-M. Doth, G. Hirzinger, and D. Rus, "Energy-efficient autonomous four-rotor flying robot controlled at 1 kHz," in *IEEE International Conference on Robotics and Automation*, April 2007, pp. 361–366.

[25] S. Lupashin, M. Hehn, M. W. Mueller, A. P. Schoellig, M. Sherback, and R. D'Andrea, "A platform for aerial robotics research and demonstration: The flying machine arena," *Mechatronics*, no. 0, pp. –, 2014.